Devil's staircase and the absence of chaos in the dc- and ac-driven overdamped Frenkel-Kontorova model

I. Sokolović,[1] P. Mali,[1] J. Odavić,[2] S. Radošević,[1] S. Yu. Medvedeva,[3,4] A. E. Botha,[5] Yu. M. Shukrinov,[3,6] and J. Tekić[7]

[1]*Department of Physics, Faculty of Science, University of Novi Sad, Trg Dositeja Obradovića 4, 21000 Novi Sad, Serbia*

[2]*Institut für Theorie der Statistishen Physik - RWTH Aachen University, Peter-Grünberg Institut and Institute for Advanced Simulation, Forschungszentrum Jülich, Germany*

[3]*BLTP, JINR, Dubna, Moscow Region, 141980, Russian Federation*

[4]*Moscow Institute of Physics and Technology, Institutsky Lane 9, Dolgoprudny, Moscow Region, 141700, Russian Federation*

[5]*Department of Physics, University of South Africa, Science Campus, Private Bag X6, Florida Park 1710, South Africa*

[6]*Department of Nanotechnology and New Materials, Dubna State University, Dubna, Moscow Region, 141980, Russian Federation*

[7]*"Vinča" Institute of Nuclear Sciences, Laboratory for Theoretical and Condensed Matter Physics – 020, University of Belgrade, P.O. Box 522, 11001 Belgrade, Serbia*

(Received 27 April 2017; published 22 August 2017)

The devil's staircase structure arising from the complete mode locking of an entirely nonchaotic system, the overdamped dc+ac driven Frenkel-Kontorova model with deformable substrate potential, was observed. Even though no chaos was found, a hierarchical ordering of the Shapiro steps was made possible through the use of a previously introduced continued fraction formula. The absence of chaos, deduced here from Lyapunov exponent analyses, can be attributed to the overdamped character and the Middleton no-passing rule. A comparative analysis of a one-dimensional stack of Josephson junctions confirmed the disappearance of chaos with increasing dissipation. Other common dynamic features were also identified through this comparison. A detailed analysis of the amplitude dependence of the Shapiro steps revealed that only for the case of a purely sinusoidal substrate potential did the relative sizes of the steps follow a Farey sequence. For nonsinusoidal (deformed) potentials, the symmetry of the Stern-Brocot tree, depicting all members of particular Farey sequence, was seen to be increasingly broken, with certain steps being more prominent and their relative sizes not following the Farey rule.

DOI: 10.1103/PhysRevE.96.022210

I. INTRODUCTION

For years, Shapiro steps, the result of dynamical mode locking of frequencies, have been the subject of intensive theoretical and experimental studies in charge-density [1–7] and spin-density [8] wave systems, vortex matter [9–11], irradiated Josephson junctions [12–16], and, more recently, even in superconducting nanowires [17,18]. As, typically, in these systems only the averaged or integrated quantities are accessible for measurement, such as current and voltage, enormous effort has been dedicated to the better understanding of the physics behind the Shapiro steps on a microscopic level. Recently, in driven colloidal systems [19], the microscopic dynamics underlying mode locking was revealed. In this case, understanding the link between the observed behavior and the microscopic dynamics of the system was a key to gaining better control over the locking of frequencies.

Externally driven systems exhibit very rich dynamics on both the macroscopic and microscopic levels. One of the models capable of capturing the essence of frequency locking, and the appearance of Shapiro steps is the Frenkel-Kontorova (FK) model under external periodic forces [20–24]. The standard FK model represents a chain of harmonically interacting identical particles subjected to the sinusoidal substrate potential [20,21]. When the external dc and ac forces are applied locking occurs between the frequency of the particles motion over the periodic potential and the frequency of external ac force [21]. On the macroscopic scale, this effect is characterized by the appearance of a staircase of Shapiro steps in the curve for average velocity as a function of the average external driving force $\bar{v}(\bar{F})$. The steps are called harmonic if the locking appears at integer multiples of the ac frequency or subharmonic at noninteger rational multiples.

Studies of Shapiro steps in the FK model have been particularly guided by the numerous theoretical and experimental results in the charge-density wave systems and the systems of Josephson junctions [20,21,24]. These systems represent typical examples of dissipative or overdamped physical systems where the inertia is irrelevant on physical grounds and where the long-term behavior is largely independent of how we start up the system [20,21,24]. For example, in the charge-density wave systems, results of numerous experiments performed on NbS_3 and TaS_3 suggested that the inertial effects were negligible [2,25,26], while in the systems of Josephson junctions, the inertial terms can be disregarded if the capacitance of junctions is small enough [12,14,27]. Detailed investigations of the overdamped Frenkel-Kontorova model have been done in Refs. [20,24,28]. The dc+ac driven standard overdamped FK model was very successful in describing harmonic locking; however, it could not be used for modeling phenomena related to subharmonic steps. Subharmonic steps do not exist in commensurate structures with integer values of winding number, while for the rational, noninteger values of winding number their size is too small, which makes analysis of their properties very difficult [29]. On the other hand, a generalization of the standard FK model, using a deformable (nonsinusoidal) substrate potential [30], does provide a good model of subharmonic frequency locking [29,31].

In general, in frequency-locking systems, there is an interesting connection between mode locking and number theory: The appearance and ordering of resonances strictly

follow the Farey rule [32]. Recently, the presence of a Farey sequence in the appearance and ordering of subharmonic steps has been shown in the FK model [33].

Understanding the stability of frequency locking in diverse physical systems, from oscillating Josephson junctions to periodically forced chicken heart cells, is intimately associated with understanding the onset of chaotic behavior [34–38]. Instead of cumbersome numerical integration of the underlying differential equations, a major breakthrough was made by the application of a one-dimensional discrete map, the "circle map," to the modeling of such systems [35,36]. Not only does the map provide a description of quasiperiodic, periodic, and chaotic behavior, but also its scaling is the same as that of a wide variety of dynamical systems that exhibit mode locking [35,36]. According to the circle map, the nonlinear systems driven by an external periodic force or field will most likely exhibit a transition to chaos caused by the overlapping of resonances, leading to the destruction of the devil's staircase [34].

Past studies of the FK model were only focused on the influence of the system parameters (amplitude and frequency of the ac force, deformation of potential, noise) on the size and existence of Shapiro steps [21]. Though these problems are very important, the complete picture about dynamical mode locking also requires an examination of possible chaotic behavior. The question whether physical systems with competing frequencies lead to a devil's staircase structure and, therefore, necessarily to chaos is of fundamental importance and may be resolved by a careful study of subharmonic steps and their properties.

In this paper, we will examine in detail the appearance and order of subharmonic Shapiro steps in the overdamped dc+ac driven Frenkel-Kontorova model, particularly focusing on the signs of chaos. High-resolution analyses of steps reveal the presence of continued fractions, i.e., the devil's staircase structure for which the fractal dimension was calculated over wide range of system parameters. However, the calculation of the largest Lyapunov exponent indicates the absence of chaotic behavior. The analysis is further extended to a model of intrinsic Josephson junctions, which confirms the disappearance of chaos as the overdamped limit is approached. Relative sizes of steps are also examined in detail for various ac amplitudes and degrees of deformation of the potential.

The paper is organized as follows. The model is introduced in Sec. II, and simulation results are presented in Secs. III–V. The devil's staircase structure is revealed and its fractal dimension is determined in Sec. III. Calculation of the largest Lyapunov exponent and an analysis of chaotic behavior in the Frenkel-Kontorova model is given in Sec. IV A. The comparative analysis of the one-dimensional (1D) stack of intrinsic Josephson junctions irradiated by electromagnetic waves is made in Sec. IV B. The relative sizes of steps are studied in Sec V. Finally, Sec. VI concludes the paper.

II. MODEL

We consider the dynamics of a series of overdamped coupled harmonic oscillators u_l, subjected to asymmetric deformable potential

$$V(u) = \frac{K}{(2\pi)^2}\frac{(1-r^2)^2[1-\cos(2\pi u)]}{[1+r^2+2r\cos(\pi u)]^2}, \tag{1}$$

where K is the pinning strength and r is deformation parameter ($-1 < r < 1$). This potential belongs to the family of nonlinear periodic deformable potentials, introduced by Remoissent and Peyrard [30] as a way to model many specific physical situations without employing perturbation methods. By changing the shape parameter r, the potential can be tuned in a very fine way, from the simple sinusoidal one for $r = 0$ to a deformable one for $0 < |r| < 1$.

The system is driven by dc and ac forces,

$$F(t) = F_{\rm dc} + F_{\rm ac}\cos(2\pi\nu_0 t), \tag{2}$$

which leads to the system of equations of motion,

$$\dot{u}_l = u_{l+1} + u_{l-1} - 2u_l - V'(u_l) + F(t). \tag{3}$$

where $l = -N/2, \ldots, N/2$; and $F_{\rm ac}$ and ν_0 are amplitude and frequency of the ac force respectively.

When the system is driven by a periodic force, two frequency scales appear: the frequency ν_0 of the external periodic (ac) force and the characteristic frequency of the particle motion over the periodic substrate potential driven by the average force $\bar{F} = F_{\rm dc}$. The competition between these two frequency scales can result in the appearance of dynamical mode locking. The solution of the system (3) is called resonant if average velocity $\bar{v}$ satisfies the relation:

$$\bar{v} = \frac{i\omega + j}{m}\nu_0, \tag{4}$$

where i, j, m are integers. The interparticle average distance (winding number) $\omega = \langle(u_{l+1} - u_l)\rangle$ is fixed to the rational or irrational value for the commensurate or incommensurate structures respectively. During their motion, the particles advance $i\omega + j$ sites during m cycles of the ac force; therefore, m represents the period of the solution, measured in the cycles of the ac force [38]. When $m = 1$, the solution corresponds to harmonic steps. If $m > 1$, then the solution is subharmonic (it includes components at the subharmonics of the ac force), and in this case, the motion is characterized by the appearance of a sequence which consists of m cycles of the ac force. Though the motion is different on each of m cycles that form the sequence, this sequence can repeat indefinitely. In the case of a commensurate structure (for which ω is rational), the resonant velocity can be written in the form $\bar{v} = \frac{i}{m}\omega\nu_0$, where the ratio $\frac{i}{m}$ marks harmonic and subharmonic steps ($\frac{i}{m} = \frac{1}{1}, \frac{2}{1}, \frac{3}{1}, \ldots$ for harmonic steps, and $\frac{i}{m} = \frac{1}{2}$ for half-integer steps).

The system (3) has been integrated by a fourth-order Runge-Kutta method with a time step of $\Delta t = 0.02/\nu_0$, supplemented with a step-doubling iteration loop until accuracy of order 10^{-8} has been achieved [39]. By comparison with more sophisticated integration methods that make use of more adaptive step size control, the global accuracy of our algorithm was consistently found to be less than 10^{-7}. We considered commensurate structures with the winding number $\omega = 1/2$

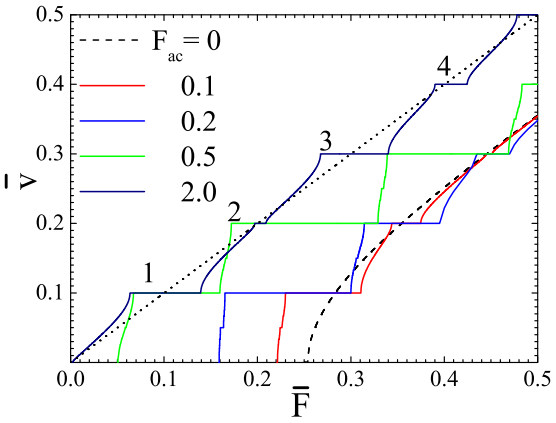

FIG. 1. The average velocity $\bar{v}$ as a function of the average driving force $\bar{F}$ for $K = 4$, $\nu_0 = 0.2$, $\omega = \frac{1}{2}$ $r = 0.01$, and different values of the ac amplitude $F_{ac} = 0, 0.1, 0.2, 0.5$, and 2 from right to left. The case $F_{ac} = 0$ corresponds to the dc-driven system represented by the dashed line while the dotted line represents linear dependence for a system of free particles. The numbers mark harmonic steps.

and varied the force adiabatically in steps ranging from $\Delta F_{dc} = 10^{-4}$ to 10^{-7}.

III. NUMBERING OF THE SUBHARMONIC SHAPIRO STEPS

The number and size of Shapiro steps which appear on the response function is determined by the amplitude of the ac force and the extent of deformation of the potential. In Fig. 1, the average velocity as a function of the average driving force is presented for various values of the ac amplitude F_{ac}, from $F_{ac} = 0$ for the dc driven system to $F_{ac} \to \infty$ for the system of free particles. Since the deformation of the potential is very small here ($r = 0.01$), the model is very close to the standard FK model, and large harmonic steps dominate in Fig. 1, at all amplitudes, while subharmonic steps are either very small or nonexistent. In the limit $F_{ac} \to 0$, the system becomes a dc-driven system, while in the opposite limit $F_{ac} \to \infty$, it becomes a system of free particles. Therefore, regardless of the value of the ac amplitude, the steps will always appear in the region of driving force which is roughly between the dc and the free particles linear curve. In their appearance, the steps are strongly correlated: Large harmonic steps correspond to small half-integer or subharmonic steps and vice versa [21] or, in other words, when some steps become large, another one must shrink.

In all frequency-locking systems, resonances always appear in a specific order. In the usual examinations of Shapiro steps in the Frenkel-Kontorova model, the locking order is not always obvious, since detection of the Shapiro steps is strongly influenced by the accuracy of the numerical procedure. However, a very high resolution in the simple analysis of the response function $\bar{v}(\bar{F})$ reveals a completely new picture of the locking phenomenon.

We will focus now on the subharmonic steps which appear between the first and the second harmonics. At the force step $\Delta F = 10^{-5}$, and in the region of the ac amplitudes where large number of well-defined steps appear, the number of

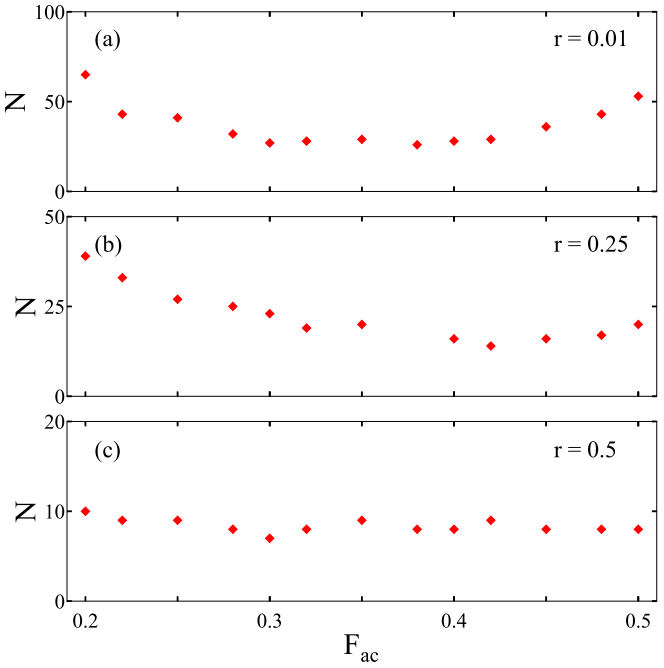

FIG. 2. Number of subharmonic Shapiro steps N detected between the first and the second harmonics at different values of the ac amplitude F_{ac} for $K = 4$, $\nu_0 = 0.2$, $\omega = \frac{1}{2}$, the force step $\Delta F = 10^{-5}$, and the three values of deformation parameter $r = 0.01, 0.25$, and 0.5 in (a), (b), and (c) respectively.

detectable subharmonic steps ranges from about 5 to 70 at different deformations as shown in Fig. 2.

We see that the extent of deformation strongly affects the number of detectable steps. The reason why more steps could not be observed at large deformation comes from the fact that the increase of r leads to appearance of very large half-integer or some other subharmonic steps [21], and since they are correlated, once some of the subharmonic steps become very large the other will shrink and become undetectable at the working resolution ($\Delta F = 10^{-5}$).

In numerical simulation, the chosen step of the driving force determines the size of the smallest step we can actually detect. Therefore, in the response functions $\bar{v}(\bar{F})$, from which the results in Fig. 2 were obtained, many of the higher-order subharmonic steps remained undetectable. However, increasing the resolution by decreasing the force step once again reveals staircase structure. In Fig. 3, the staircase structure of the average velocity as a function of the average driving force $\bar{v}(\bar{F})$ is presented for $\Delta F = 10^{-7}$.

If we consider the section between the first and the second harmonic step in Figs. 3(a) and 3(b), then we could see a large half-integer step $\frac{3}{2}$ and some subharmonic steps between $\frac{3}{2}$ and 2. Though it might seem that there are no subharmonic steps between 1 and $\frac{3}{2}$, further magnification in Figs. 3(c) and 3(d) once more reveals the devil's staircase structure.

If we increase the ac amplitude F_{ac}, then the number of harmonic steps significantly increases. In Fig. 4, the staircase structure of the response function $\bar{v}(\bar{F})$ is presented for large amplitudes of the ac force.

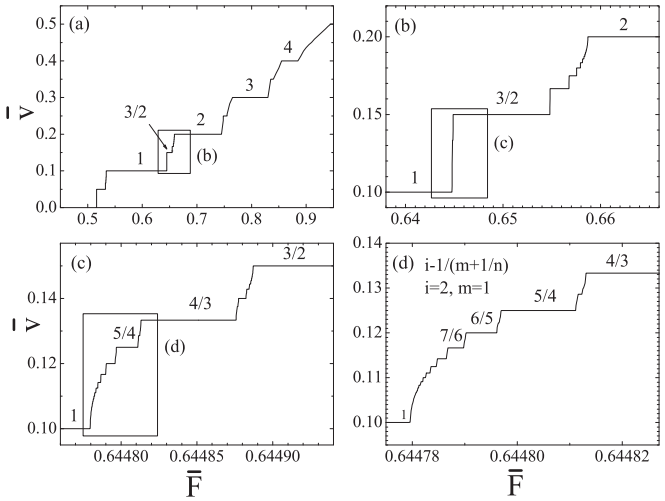

FIG. 3. The average velocity as a function of the average driving force $\bar{v}(\bar{F})$ for $K = 4$, $\nu_0 = 0.2$, $\omega = \frac{1}{2}$, $r = 0.5$, and $F_{ac} = 0.2$. Numbers mark harmonic and subharmonic steps. The devil's staircase in (b), (c), and (d) represent the high-resolution views of the selected areas in (a), (b), and (c), respectively.

As in the case of Fig. 3, magnification of the steps between the first and the second harmonics in Fig. 4(a) shows that an infinite series of subharmonic steps start to appear in Figs. 4(b), 4(c) and 4(d).

It was shown that in the dc+ac-driven FK model, all observable subharmonic Shapiro steps belong to various Farey sequences without exceptions [33]. Farey sequence of the order n consists of all the irreducible fractions between 0 and 1 whose denominator is less or equal to n: $0 \leqslant h \leqslant k \leqslant n$, $(h,k) = 1$. If we extend this statement to the case of the interval between

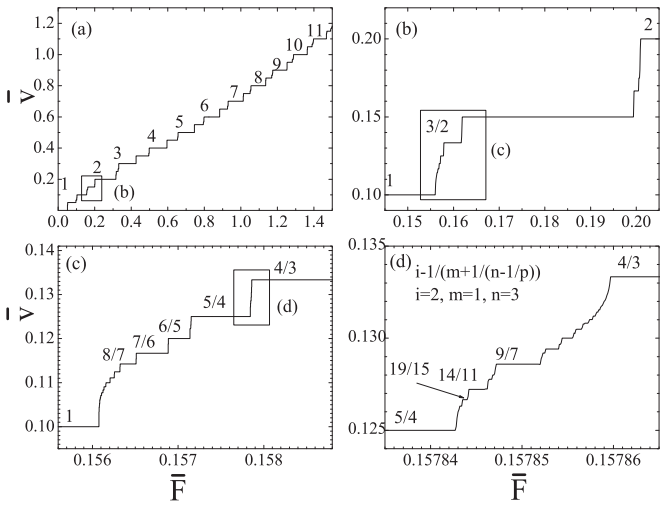

FIG. 4. The average velocity as a function of the average driving force $\bar{v}(\bar{F})$ for $K = 4$, $\nu_0 = 0.2$, $\omega = \frac{1}{2}$, $r = 0.5$, and $F_{ac} = 1.1$. Numbers mark harmonic and subharmonic steps. The devil's staircase in (b), (c), and (d) represent the high-resolution views of the selected areas in (a), (b), and (c), respectively.

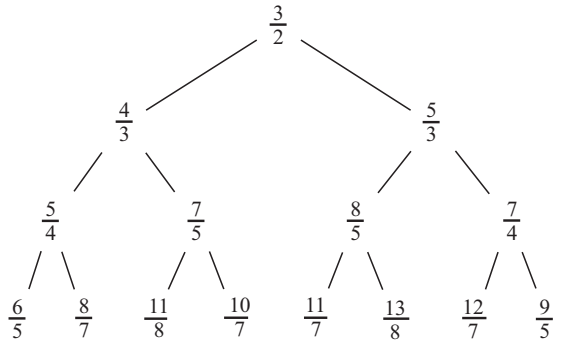

FIG. 5. Part of the Stern-Brocot tree depicting all the members of Farey sequence $\mathcal{F}_5$ and some members of higher Farey sequences. Fractions corresponding to the integers $\frac{1}{1}$ and $\frac{2}{1}$ are not shown in the figure. Fraction $\frac{3}{2}$ represents the root or starting node of the tree.

1 and 2, then the first five Farey sequences are given by

$$\begin{aligned}
\mathcal{F}_1 &= \left\{\tfrac{1}{1}, \tfrac{2}{1}\right\},\\
\mathcal{F}_2 &= \left\{\tfrac{1}{1}, \tfrac{3}{2}, \tfrac{2}{1}\right\},\\
\mathcal{F}_3 &= \left\{\tfrac{1}{1}, \tfrac{4}{3}, \tfrac{3}{2}, \tfrac{5}{3}, \tfrac{2}{1}\right\},\\
\mathcal{F}_4 &= \left\{\tfrac{1}{1}, \tfrac{5}{4}, \tfrac{4}{3}, \tfrac{3}{2}, \tfrac{5}{3}, \tfrac{7}{4}, \tfrac{2}{1}\right\},\\
\mathcal{F}_5 &= \left\{\tfrac{1}{1}, \tfrac{6}{5}, \tfrac{5}{4}, \tfrac{4}{3}, \tfrac{7}{5}, \tfrac{3}{2}, \tfrac{8}{5}, \tfrac{5}{3}, \tfrac{7}{4}, \tfrac{9}{5}, \tfrac{2}{1}\right\}.
\end{aligned} \tag{5}$$

If we have two rational fractions $\frac{p}{q}$ and $\frac{p'}{q'}$ where p, q, p', q' are coprime integers, then the next member of a Farey sequence is generated according to median rule given as:

$$\frac{p}{q} \oplus \frac{p'}{q'} = \frac{p+p'}{q+q'}. \tag{6}$$

Therefore, if the fractions $\frac{p}{q}$ and $\frac{p'}{q'}$ were neighbors in the Farey sequence $\mathcal{F}_{n-1}$, then they will be separated by the fraction $\frac{p+p'}{q+q'}$ in the Farey sequence $\mathcal{F}_n$, where $(q + q')$ is smaller or equal to n. Farey sequences can be defined between any two integers k and $k + 1$ by translating the original Farey sequence along the real number axis by the value of the integer $k > 0$.

Members of the Farey sequences can be represented using the Stern-Brocot (SB) tree as shown in the Fig. 5. The SB tree is an infinite complete binary tree which consists of all the rational numbers between two given integers k and $k + 1$. The connection between Farey sequences and the SB tree is that the new members of the SB tree are created by the median rule given in Eq. (6). The SB tree contains all the fractions which belong to these Farey sequences. In Fig. 5, it is expanded up to the fourth level, so that all members of $\mathcal{F}_5$ are present in the tree. One can notice that in order to reach all the members of the fifth Farey sequence, one must construct a tree with a plethora of fractions, many of which belong to higher Farey sequences. If we draw a vertical line passing through the only node of the first level of the SB tree ($\frac{3}{2}$), and not through any other node of the infinite binary tree, then such a line could be considered a symmetry axis of the SB tree. Fractions that are symmetric with respect to this axis have the same denominator and they are arithmetically symmetric.

In the devil's staircase structure, the steps appear following the continued fraction formula [15], which in the case of the ac driven FK model can be written as:

$$\bar{v} = \left(i \pm \frac{1}{m \pm \frac{1}{n \pm \frac{1}{p \pm \ldots}}} \right) \omega \nu_0, \tag{7}$$

where $i,m,n,p,\ldots$ are positive integers. Harmonic steps are presented by the first-level terms, which involve only i, while the other terms involving other integers describe subharmonic or fractional steps. Terms involving i and m are called second-level terms, those with i, m, and n third-level terms, etc. If we look the results in Fig. 3 and Fig. 4, then we can see that the subharmonic steps $\frac{1}{2}, \frac{2}{3}, \frac{3}{2}, \frac{4}{3}, \ldots$ represent second-level steps created by the formula $i - \frac{1}{m}$ or $(i-1) + \frac{1}{m}$ for $i = 2$. In Figs. 3(d) and 4(c), the steps $\frac{4}{3}, \frac{5}{4}, \frac{6}{5}, \frac{7}{6}, \ldots$ are sequences of the third level, while in Fig. 4(d), the fractions of the fourth level $\frac{9}{7}, \frac{14}{11}, \frac{19}{15}, \ldots$ are clearly visible. An increase in resolution reveals more and more subharmonic steps, belonging to higher levels of continued fractions. Therefore, the average velocity as a function of average driving force exhibits the devil's staircase of infinite but countable steps (resonances), which can be reproduced by continued fractions formula in Eq. (7). Between any two steps there is an infinity of steps, and it is this property that has given rise to the name "the devil's staircase" [34]. This progressive generation of subharmonic steps within devil's staircase is a manifestation of its self-similarity [15].

In frequency-locking systems, the locking appears at an infinity of driving frequencies, giving rise to steps with a characteristic scaling dimension; the so-called fractal dimension between 0 and 1 [34]. In the dynamical-locking of the FK model, the fractal dimension has been calculated for different system parameters. To investigate the completeness of the staircase, we consider the region between the first and the second harmonics whose length can be written as $L = \min F_{2\mathrm{dc}} - \max F_{1\mathrm{dc}}$, where $\min F_{2\mathrm{dc}}$ corresponds to the value of dc force where the second harmonic appears, while $\max F_{1\mathrm{dc}}$ marks the end of the first harmonic step. If we measure the total length $S(l)$ of all steps larger than l, where l is taken arbitrary, then the missing intervals between the steps have total length $L - S(l)$. We define $N(l)$ as this length measured in the scale l, i.e., $N(l) = [L - S(l)]/l$. For complete locking $lN \to 0$ as $l \to 0$:

$$N(l) \sim \left(\frac{1}{l}\right)^D, \tag{8}$$

where D represents the fractal dimension.

If we consider the the results in Fig. 2, then for that region of parameters and accuracy, we obtain the fractal dimension D presented in Fig. 6. For smaller deformations $r = 0.01$ or 0.25, it changes around 0.87, which is presented by a dashed line in Fig. 6, while the further increase of r causes a definite decrease of the fractal dimension, as can be seen for $r = 0.5$.

An example of our calculation of the fractal dimension (for a small deformation $r = 0.01$, for which the FK model is very close to the standard model) is presented in Fig. 7. Here $\log_{10}[N(l)]$ as a function of $\log_{10}(\frac{1}{l})$ is plotted with the corresponding staircase structure between the first and the second harmonics (in the inset).

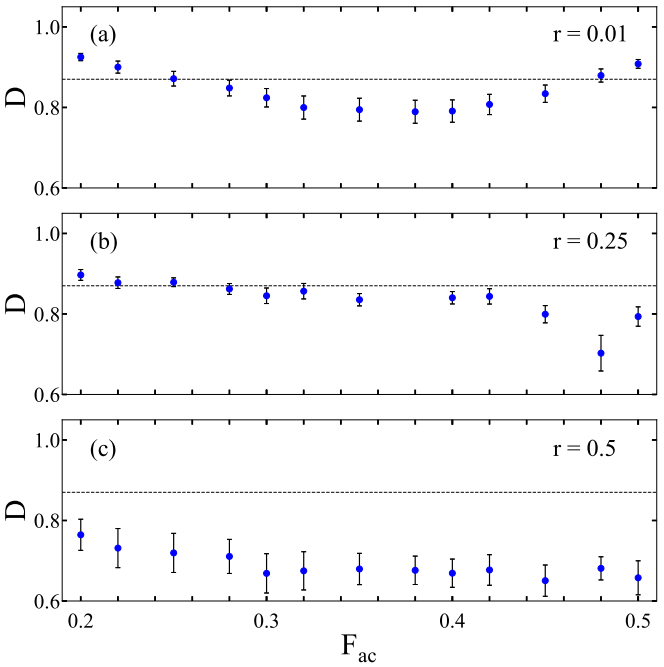

FIG. 6. Fractal dimension D as a function of the ac amplitude F_{ac} for $K = 4$, $\nu_0 = 0.2$, $\omega = \frac{1}{2}$; the force step $\Delta F = 10^{-5}$; and $r = 0.01, 0.25$ and 0.5 in (a), (b), and (c) respectively. The dash line marks the value $D = 0.87$.

The points are almost exactly linear, confirming the power-low dependence given in Eq. (8), with the fractal dimension $D = 0.862$.

IV. IN SEARCH FOR CHAOS

It is well known that dissipative dynamical systems with competing frequencies can be described by the circle map, which has a cubic inflection point. Depending on the strength of the coupling, such systems will exhibit the devil's staircase and a transition to chaos [34–36]. When the coupling is

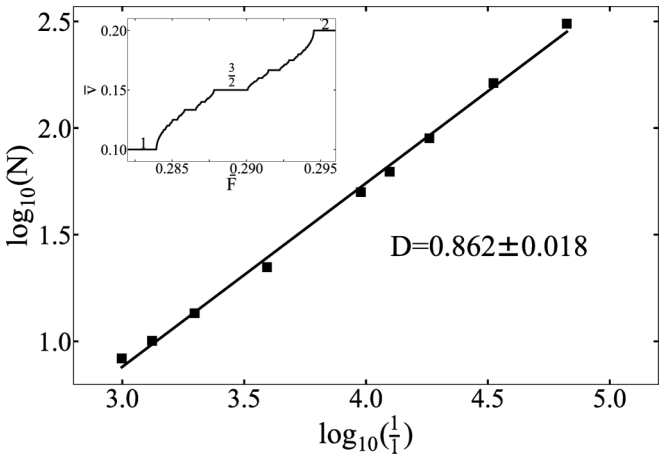

FIG. 7. Plot of $\log_{10} N(l)$ vs $\log_{10}(\frac{1}{l})$ for $K = 4$, $\nu_0 = 0.2$, $\omega = \frac{1}{2}$, $r = 0.01$, and $F_{\mathrm{ac}} = 0.25$. The slope determines the fractal dimension D. The inset shows the corresponding region between the first and the second harmonic steps.

below some critical value, the staircase is *incomplete*, i.e., there are quasiperiodic intervals between the frequency locked plateaus (steps) of periodic behavior. As coupling increases, the frequency locked regions start to spread, and at some critical value, they fill up all the space. The quasiperiodic intervals have zero measure, and the devil's staircase is said to be *complete*. The most striking property of the devil's staircase is that, though the quasiperiodic intervals have zero measure, they have nonzero fractal dimension (scaling index) which is *universal*, i.e., the same $D = 0.87$ for all the systems (at least for those described by the circle map with a cubic inflection point), and thus often considered as a constant of nature [34]. The mechanism leading eventually to chaos is the interaction between different resonances caused by the nonlinear coupling and overlapping of resonant regions when coupling exceeds certain critical value.

However, the universality of this scenario as well as the universality of the fractal dimension ($D = 0.87$) have been questioned in the past few years. Numerous theoretical and experimental studies in the wide range of biological, chemical, and physical systems have been devoted to models showing the occurrence of entire nonchaotic regions with complete phase locking [40–43]. Nonchaotic transition from quasiperiodicity to complete locking [40] and *deviation from the universality* with fractal dimension varying from 0.64 to 0.98 have been observed [42,44]. In those systems, transition to complete locking is separated from the transition to chaos, and these nonchaotic systems with two competing frequencies will exhibit a strong mode-locking structure with a scaling properties similar to those of a quasiperiodic systems near transition to chaos [41]. The classic scenario of transition to chaos via the usual mechanism of resonance overlap has been also questioned. The chaotic dynamics does not appear due to locking on invariant torus but rather due to the map developing two extrema [45].

A. The overdamped Frenkel-Kontorova model

In order to examine chaotic behavior, we will apply the largest Lyapunov exponent (LE) computational technique and extend our examination to a very high resolution and wider range of parameters, the ac amplitudes in particular. As in our previous work [33], for the calculation of the largest Lyapunov exponent we use the technique given in Ref. [46]. In Fig. 8, the largest Lyapunov exponent for the standard FK model ($r = 0$) is presented as a function of driving force for very high values of the ac amplitude. Each negative minima of the LE corresponds to the step, i.e., resonance in the plot $\bar{v}(\bar{F})$ for the same values of driving force. These results clearly show the absence of chaos since the LE remains always negative regardless of the applied force. In our search for chaos, the other methods have been also applied. The same conclusion was reached independently by performing the full spectrum calculation [47] at a variety of parameter combinations. The other technique, such as the calculation of the smallest alignment index (SALI) [48,49] also confirmed the absence of chaos.

The absence of chaos in the ac driven overdamped FK model can be attributed to the dissipative character of the system and the Middleton no-passing rule [50,51]. According

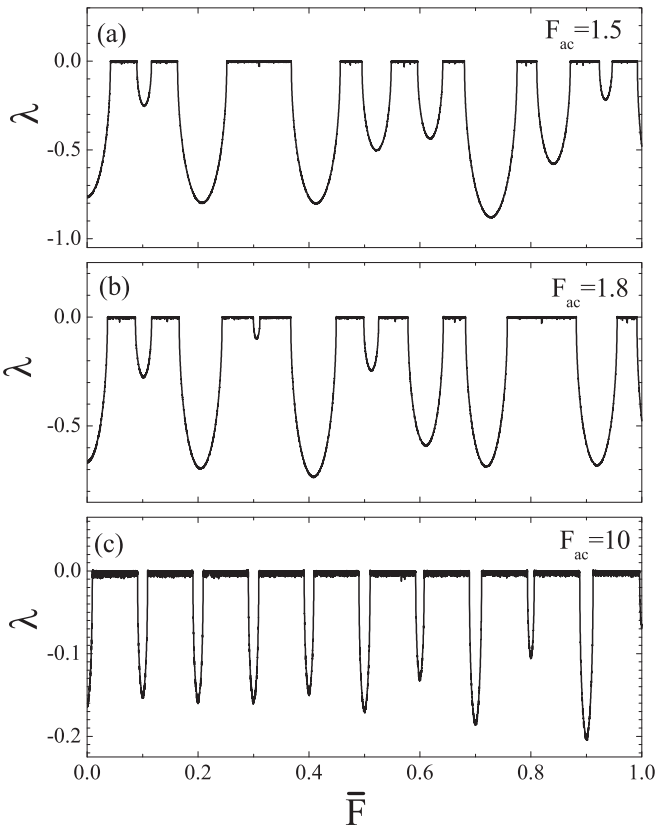

FIG. 8. The largest Lyapunov exponent as a function of the ac amplitude $K = 4$, $\nu_0 = 0.2$, $\omega = \frac{1}{2}$, and $F_{ac} = 1.5$, 1.8, and 10 in (a), (b), and (c), respectively.

to this rule which applies strictly on overdamped systems, the order of particles must be preserved in dynamics or, in other words, the particles cannot jump over each other while they move. In such case, there could be no overlapping of resonances which is the main cause of the chaotic behavior in frequency-locking systems [16,34–36]. Also, while in many systems the increase of the ac amplitude leads the system to chaos [15,16,37,38], it could also have completely opposite effect: The increase of the ac amplitude to very high values decouples particles turning the model into a system of free particles in which case there can be no chaotic behavior.

B. The system of Josephson junctions

Numerous experimental and theoretical works on chaos have been performed in physical systems related to the Frenkel-Kontorova model [5]. (A good overview of the past studies can be found in Ref. [15,16] and references therein.) Structured chaos in the devil's staircase has been recently observed both in numerical simulations of the single Josephson junction [15,16] and 1D stacks of of intrinsic Josephson junctions, irradiated by electromagnetic waves [52]. There, as in the present work, the resonant dynamics is characterized by the existence of a devil's staircase, where the heights of the steps may be determined by the continued fraction formula. In the system of Josephson junctions, the subharmonic steps were separated by structured chaotic windows. One of the system parameters which played a key role as a control parameter for

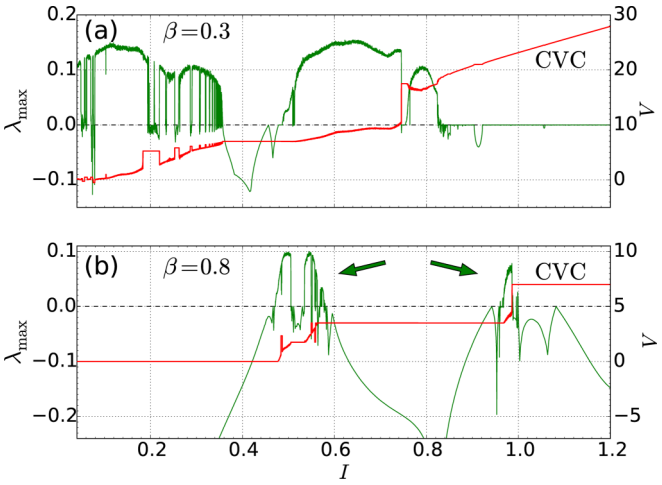

FIG. 9. I-V characteristics and corresponding maximal Lyapunov exponent for a stack of seven intrinsic Josephson junctions, simulated from Eqs. (9), with $N = 7$, $\alpha = 0.1$, $A = 0.8$, $\omega_{\rm rf} = 0.5$, and at two different values of dissipation parameter $\beta = 0.3$ and 0.8 in (a) and (b), respectively. The dashed lines correspond to the zero value of LE, while the arrows in (b) indicate the chaotic regions that appear between adjacent Shapiro steps.

the onset of the structured chaos was the ac amplitude of the external radiation [15,16,37,38].

In this section, we will perform a comparative analysis of the present system in comparison to the chaotic behavior that has been studied in 1D stacks of intrinsic Josephson junctions under external radiation. The dynamics of the latter system is described by the coupled equations:

$$\dot{V}_l = I - \sin\varphi_l - \beta\dot{\varphi}_l + A\sin(\omega_{\rm rf}t), \tag{9a}$$

$$\dot{\varphi}_l = V_l - \alpha(V_{l+1} + V_{l-1} - 2V_l), \tag{9b}$$

where φ is the phase difference, α is the capacitive coupling between junctions, and β represents the damping (dissipation) parameter, while A and $\omega_{\rm rf}$ are the amplitude and frequency of external radiation, respectively. Linearization of the uncoupled ($\alpha = 0$) equations shows that the system is underdamped for $\beta < 2$, critically damped for $\beta \approx 2$, and overdamped for $\beta > 2$.

Previously, the current-voltage (IV) characteristic of this system was studied in the underdamped case [52]. Over a certain range of parameters, the system was found to contain a devil's staircase, interspaced with self-similar chaotic windows that preserve the scaling properties of the complete staircase [52]. In the present work we employ the Lyapunov exponent (LE) computational technique from Ref. [47] to examine the chaotic behavior of the system at different levels of damping. In Fig. 9, the IV characteristic and the corresponding values of the maximal Lyapunov exponent are presented for the stack of $N = 7$ Josephson junctions at two different values of dissipation parameter. By comparing the values for the LE in Figs. 9(a) and 9(b), one can clearly see that an increase of dissipation significantly reduces the tendency for chaos to occur in this system.

Extending further our analysis to wider range of dissipation, the maximal Lyapunov exponent, as a function of the dc bias current I and the damping β, is presented in Fig. 10. The black regions in Fig. 10 correspond to zero LE and, therefore, the absence of chaos. Notice that in this system the maximal LE is always positive, or else zero, because in any continuous time-dependent dynamical system without a fixed point there is a zero exponent corresponding to the slowly changing magnitude of a principal axis tangent to the flow [47].

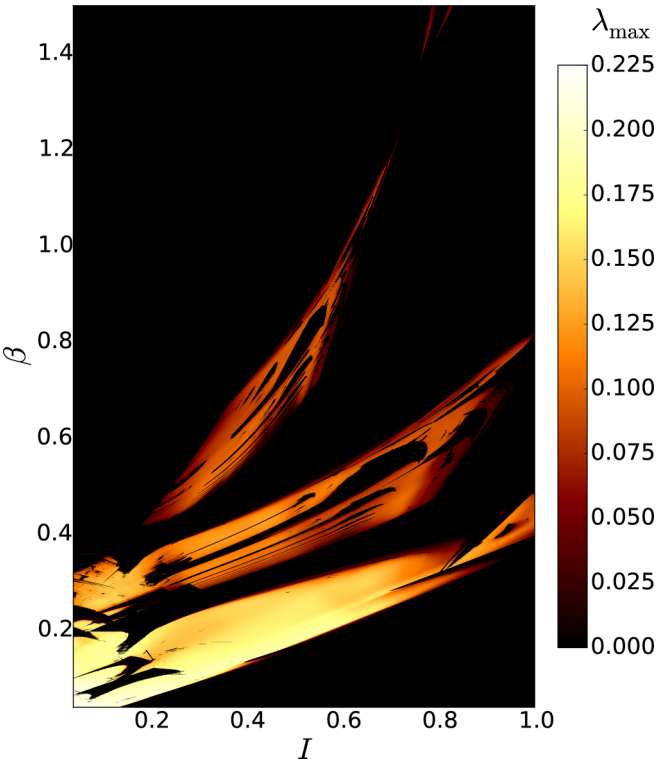

FIG. 10. Maximal Lyapunov exponent as a function of the bias current I and damping parameter β, for the stack of seven junctions. All other parameters are the same as in Fig. 9.

The results in Figs. 9 and 10 clearly demonstrate the disappearance of chaotic behavior in the 1D stack of Josephson junctions with increasing dissipation. It is important to point out that the FK model studied here has many degrees of freedom, as does the Josephson junction systems. Thus the absence of chaos in the overdamped FK model cannot be ascribed to a reduction in the effective dimensionality of the system.

V. RELATIVE SIZES OF SHAPIRO STEPS

In this section, we will examine the relative sizes of the Shapiro steps and the critical depinning force. The Stern-Brocot tree presented in Fig. 5 provides another insight into the steps widths as follows: subharmonic Shapiro steps which appear in lower branches of the SB tree have smaller size than steps belonging to higher branches. By lower and higher branches of the tree we are addressing the branches that are further or closer to the root of the tree $\frac{3}{2}$, respectively. This rule, combined with the rule of denominator increase, governs the step widths, i.e., steps are smaller if denominator is larger, and if they belong to lower branches.

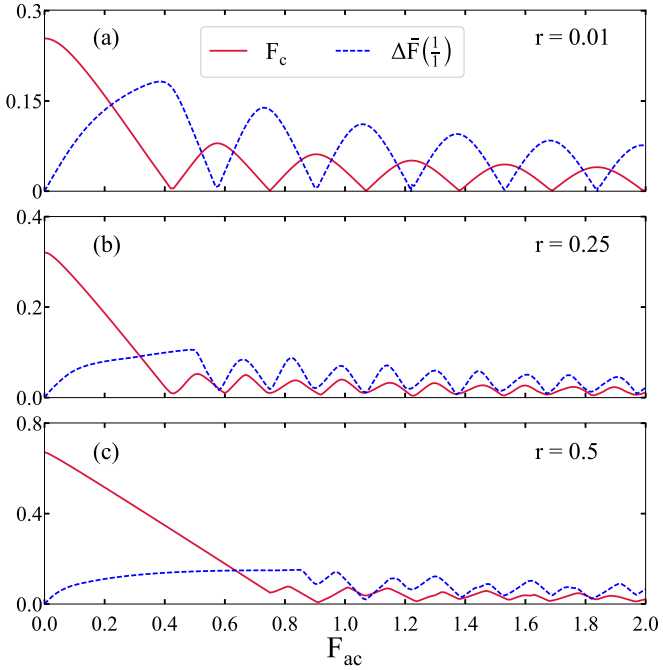

FIG. 11. Critical depinning force F_c and the width ΔF of first harmonic Shapiro step $\frac{1}{1}$ as a function of the ac amplitude F_{ac} for $K = 4$, $\nu_0 = 0.2$, $\omega = \frac{1}{2}$, and different values of deformation parameter $r = 0.01, 0.25$, and 0.5 in (a), (b), and (c) respectively.

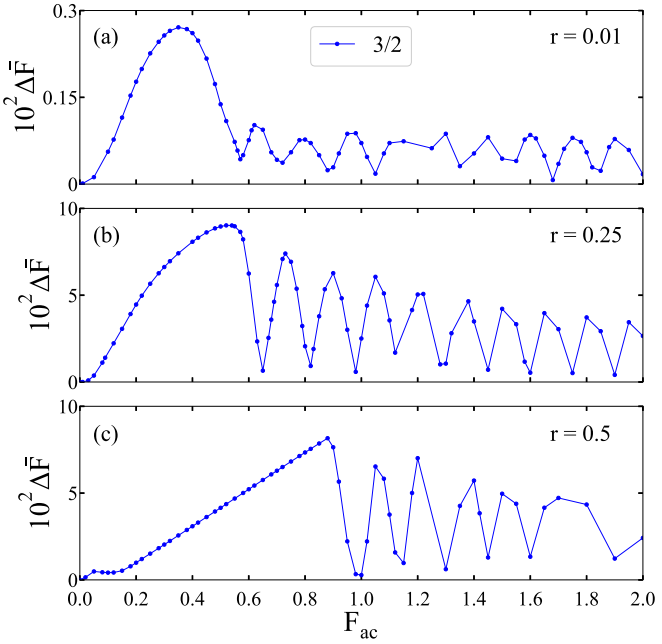

FIG. 12. The width ΔF of the halfinteger Shapiro step $\frac{3}{2}$ as a function of the ac amplitude F_{ac}. The rest of parameters are the same as in Fig. 11.

1. *Harmonic steps and the critical depinning force*

The critical depinning force and the width of first harmonic Shapiro step as a function of the ac amplitude F_{ac} for different deformations of the substrate potential are shown in Fig. 11.

Critical depinning force in the ac+dc driven Frenkel-Kontorova model is the uniform force necessary for the system of particles to exhibit collective motion [23]. It is well known that the size of the first harmonic step and critical depinning force exhibit Bessel-like oscillations where maxima of one curve correspond to minima of another [21].

It was shown previously [31] that as deformation increases, the system evolves through different types of amplitude dependence. For small deformation $r = 0.01$ in Fig. 11, we have typical standard behavior where the first harmonic step and the critical depinning force oscillate in counterphase, i.e., minima of one curve corresponds to the maxima of another. As deformation increases for $r = 0.25$ and $r = 0.5$, the oscillations get into phase and the Bessel form is lost (oscillations became anomalous where the third lobe is higher than the second, etc.).

2. *Half-integer step* $\frac{3}{2}$

According to the Farey construction, the first subharmonic step that appears between the first and second harmonics is the half-integer step $\frac{3}{2}$. The influence of the ac amplitude on its size is presented in the Fig. 12.

The steps with a higher denominator should have the smaller relative sizes than the steps with lower denominator [32]. This implies that the largest subharmonic step in the region between the first and the second harmonics is the step $\frac{3}{2}$. In contrast to that rule of descending step size with the ascending denominator value, in Figs. 11 and 12, when $r = 0.25$ the size of the step $\frac{3}{2}$ can be larger than the size of the first harmonic. As we can see from Fig. 12, even at the smallest value of deformation parameter $r = 0.01$, the oscillations do not have Bessel-like form since the maxima of oscillations do not decrease monotonously (the third maximum is lower than the fourth one). It appears that this property which was apparent at the oscillations of the first harmonic is lost as we progress to higher Farey sequences.

At the value of deformation parameter $r = 0.25$ for which the width of the step $\frac{3}{2}$ is greater than the width of the step $\frac{1}{1}$, clear Bessel-like oscillations of the step $\frac{3}{2}$ are present while the first harmonic exhibits anomalous oscillations. Based on this observation, we conclude that Bessel-like oscillations of the steps, at deformation parameter $r = 0.25$, will appear only at the more pronounced step of the two. If the system is subjected even to the higher deformation parameter $r = 0.5$, then the both steps (harmonic and fractional) exhibit anomalous oscillations.

3. *Subharmonic steps* $\frac{4}{3}$ *and* $\frac{5}{3}$

Two new steps emerge once we progress to the higher Farey sequence $\mathcal{F}_3$ or the lower level of the SB tree. These are the steps $\frac{4}{3}$ and $\frac{5}{3}$ which represent a symmetric pair on the SB tree in Fig. 5. The amplitude dependence of subharmonic steps $\frac{4}{3}$ and $\frac{5}{3}$ at different deformations of the substrate potential is shown in the Fig. 13.

In the standard case or when deformation is small $r = 0.01$, both steps $\frac{4}{3}$ and $\frac{5}{3}$ have the same size at the small ac amplitudes. As F_{ac} increases to the higher values, the steps start to oscillate in counter phase (the maxima of one corresponds to the minima of another), and they are of the same magnitude compared to each other. As deformation increases to $r = 0.25$,

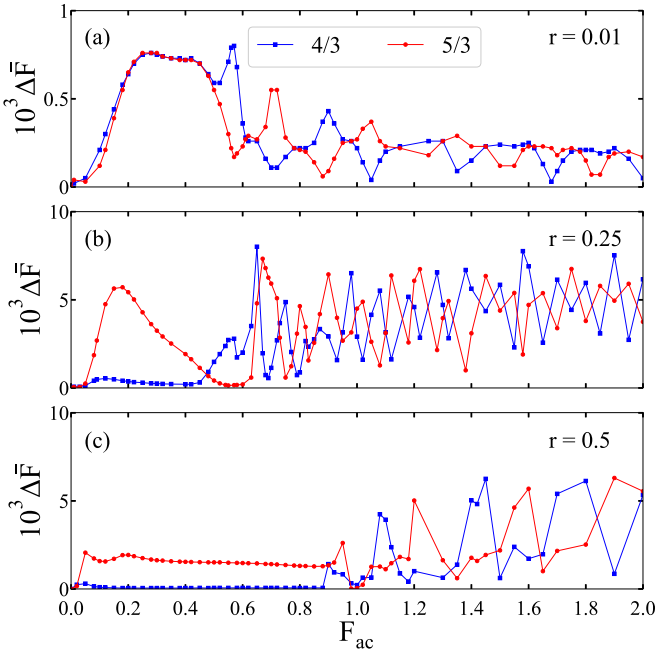

FIG. 13. The width ΔF of the Shapiro step $\frac{4}{3}$ and $\frac{5}{3}$ as a function of the ac amplitude F_{ac}. The rest of parameters are the same as in Fig. 11.

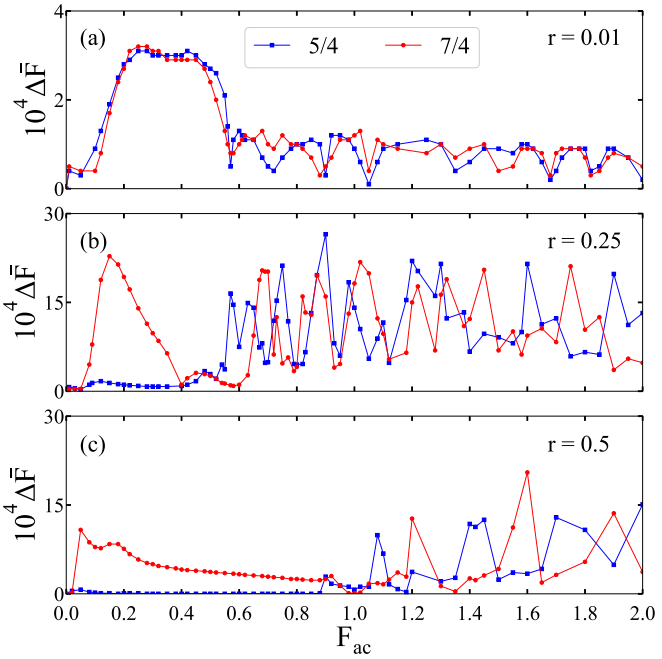

FIG. 14. The width ΔF of the Shapiro step $\frac{5}{4}$ and $\frac{7}{4}$ as a function of the ac amplitude F_{ac}. The rest of parameters are the same as in Fig. 11.

the symmetry between subharmonic steps $\frac{4}{3}$ and $\frac{5}{3}$ disappears. Though both steps belong to the same level of the SB tree in Fig. 5, there is a clear dominance of the step $\frac{5}{3}$ over the step $\frac{4}{3}$ in lower range of F_{ac}. As in the standard case for $r = 0.01$, further increase of the ac amplitude will induce oscillatory behavior where steps oscillate in counter phase with the similar magnitudes. When the substrate potential deviates greatly from the perfectly symmetric sinusoidal potential such as for $r = 0.5$, the region of F_{ac} in which the step $\frac{5}{3}$ dominates the step $\frac{4}{3}$ is spread to the higher amplitudes. For larger amplitudes $F_{ac} > 1$, both steps again oscillate in counter phase with the significant increase in magnitude of oscillations with F_{ac}. As in the case for fractional step $\frac{3}{2}$ in Fig. 12, we can see that in Fig. 13 the size of steps is the smallest in the standard case when $r = 0.01$, it reaches the largest values at $r = 0.25$, and declines as r is increased to $r = 0.5$.

According to these results it is obvious that the asymmetry of the substrate potential favors some steps as it was indicated in Ref. [33]. However, this favorable pronunciation is limited to a lower range of F_{ac} after which, at the higher amplitudes, the steps seem to be equally influenced by the amplitude of the oscillatory force.

4. Subharmonic steps $\frac{5}{4}$ and $\frac{7}{4}$

Farey sequence $\mathcal{F}_4$ differs from $\mathcal{F}_3$ by two fractions: $\frac{5}{4}$ and $\frac{7}{4}$. These two steps are on the third level of the SB tree, and they are symmetric to the vertical axis of the tree. Amplitude dependence of subharmonic steps $\frac{5}{4}$ and $\frac{7}{4}$ for different deformation of substrate potential is presented in Fig. 14. Again, at small deformation $r = 0.01$, the steps are similar to each other in size, and only in this case, the maximum of the first lobe is larger than other maxima. Though the steps oscillate there is no similarity with the Bessel-like oscillations which appears to be lost with the increase in denominator. This degradation of the Bessel-like shape is followed by an increase in the oscillation complexity. It seems that the Bessel-like shape of oscillations becomes more distorted (more anomalous) as the denominator of the steps increases, which could be attributed to the significant decrease of the absolute widths when compared to other subharmonic steps with smaller denominator.

Increase in deformation to the values $r = 0.25$ and $r = 0.5$ induces a clear pronunciation of the step $\frac{7}{4}$ in the region of low amplitudes F_{ac}. As in the case with the steps whose denominators were equal to 3 in Fig. 12, only the step with the higher numerator is present in the first region. Both steps $\frac{5}{3}$ and $\frac{7}{4}$ belong to the right-hand side of the SB tree. Dominance of only some subharmonic step from the same level of SB tree is not present in the standard case or at the small deformations such as $r = 0.01$, and, thus, it is surely induced by the increase in asymmetry of the substrate potential. As amplitude increases, in the second region, the steps start to oscillate becoming comparable in magnitude.

5. Subharmonic steps $\frac{6}{5}$, $\frac{7}{5}$, $\frac{8}{5}$, and $\frac{9}{5}$

With further increase in the denominator value, there are four possible irreducible fractions between 1 and 2: $\frac{6}{5}$, $\frac{7}{5}$, $\frac{8}{5}$, and $\frac{9}{5}$. Each of these fractions is a member of the $\mathcal{F}_5$ Farey sequence, and we have observed subharmonic Shapiro steps which correspond to the complete $\mathcal{F}_5$ sequence. Unlike the subharmonic steps which we presented so far, the transition from $\mathcal{F}_4$ to $\mathcal{F}_5$ creates fractions which do not belong on the same level of the SB tree.

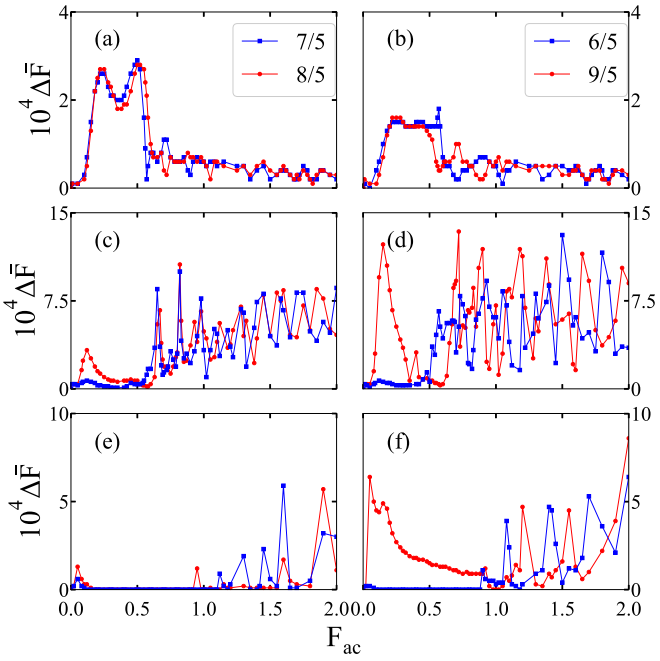

FIG. 15. The width ΔF of the Shapiro steps of subharmonic Shapiro steps with denominator being equal to 5 as a functions of the ac amplitude F_{ac}. The rest of parameters are the same as in 11.

Amplitude dependence of each subharmonic step with denominator equal to 5 for different deformation of the substrate potential is shown in Fig. 15. The left-hand side of the figure compares the steps $\frac{8}{5}$ and $\frac{7}{5}$ which are in the third level of the SB tree, while the right-hand side compares the steps $\frac{6}{5}$ and $\frac{9}{5}$ from the fourth level. Both comparisons are performed on the steps which form a symmetric pair, i.e., they are symmetric to each other in respect to the vertical axis of the SB tree.

In the standard case when deformation is small $r = 0.01$, the side-by-side comparison in the Fig. 15 shows that the steps which form a symmetric pair on the SB tree have similar sizes and similar amplitude dependence. As deformation of the potential increases, for $r = 0.25$ and $r = 0.5$, only two of the four steps are present in the first region of small F_{ac}. These are the steps with higher numerator $\frac{8}{5}$ and $\frac{9}{5}$. The step $\frac{9}{5}$ is greater in magnitude than the step $\frac{8}{5}$ in this range of F_{ac}, implying that the larger the numerator the larger the step with the same denominator. As amplitude increases, in the second region, all four steps are equally pronounced, where the steps from the same symmetric pairs of the SB tree have similar sizes. We can clearly see in Fig. 15 that in the standard case ($r = 0.01$) the steps $\frac{7}{5}$ and $\frac{8}{5}$ from the third level of SB tree are larger than the steps $\frac{6}{5}$ and $\frac{9}{5}$ from the fourth one. However, this is not the case when potential becomes deformed; for $r = 0.25$ and $r = 0.5$ the steps $\frac{6}{5}$ and $\frac{9}{5}$ from the fourth level of the SB tree are much larger than the steps $\frac{7}{5}$ and $\frac{8}{5}$ from the third one.

The presented results in Figs. 11–15 clearly show that relative sizes of the steps do not necessarily follow the Farey rule. If we look for instance the steps $\frac{4}{3}$ in Fig. 13 and $\frac{7}{4}$ in Fig. 14, contrary to the Farey rule, the step $\frac{7}{4}$ is larger than the step $\frac{4}{3}$ when potential is deformed which is particularly obvious in the first region of F_{ac}. Similar examples could be found also for other subharmonic steps ($\frac{9}{5}$ can be larger than $\frac{5}{4}$, even $\frac{4}{3}$).

6. *Breaking of symmetry*

From the presented results it has become clear that all subharmonic Shapiro steps can be described in a somewhat similar manner. Namely, depending on the deformation of the potential for all subharmonic steps we could distinguish two different regions in their dependence of the ac amplitude:

(i) *The first region or the low-amplitude region* corresponds to the first lobe or the first maximum of the step size in Figs. 11–15. In the standard case, in this region, the subharmonic steps which form the symmetric pair on the Stern-Brocot tree have the same size. With the increase of deformation, however, the one with the larger numerator becomes dominant. This region spreads to the higher amplitudes as deformation increases.

(ii) *The second or oscillatory region* corresponds to the higher ac amplitudes. In this region, both members of each symmetric pairs in SB tree oscillate in counterphase with the similar magnitudes.

Therefore, in the FK model with asymmetric deformable potential, increase of deformation breaks the symmetry of the Stern-Brocot tree in a way that in the first region, at the lower ac amplitudes, the steps from the right-hand side of the SB tree are clearly pronounced in favor of those from the left-hand side. In the second region with the increase of the ac amplitude, this symmetry is again established. There is no indication that there are limitations on the upper bound of the range of the second region.

VI. CONCLUSION

In this work, a high-resolution numerical analysis of the Frenkel-Kontorova model driven by time periodic forces has been made. We have shown the presence of a devil's staircase in the average velocity as a function of the average driving force. The hierarchical ordering of the Shapiro steps has been presented in terms of continued fraction formula, and the fractal dimension has been calculated. However, contrary to the well-known scenario from the circle map, where the staircase only becomes complete immediately before the onset of chaos, *no chaotic behavior* has been detected. The absence of chaos is a result of the overdamped character of the FK model and, above all, "the Middleton no-passing rule." The comparative study of the 1D stacks of intrinsic Josephson junctions irradiated by electromagnetic waves has confirmed the disappearance of chaos as the system becomes overdamped. Other common dynamical features have also been identified through this comparison. A detail examination of the amplitude dependence of the Shapiro steps has revealed that only for the case of a purely sinusoidal substrate potential do the relative sizes of the steps follow a Farey sequence. As the substrate potential becomes deformed, the symmetry of the Stern-Brocot tree, depicting all members of particular Farey sequence, becomes increasingly broken; certain steps being more prominent, and their relative sizes not following the Farey rule.

This work could be important to all frequency locking systems, but particularly to those related to the overdamped Frenkel-Kontorova model, such as charge- or spin-density wave systems, vortex latices, and the systems of Josephson-junction arrays [21]. Shapiro steps and interference phenomena are significant for technological applications and, therefore, situations in which the parameters should be set to produce desired dynamical effects without evoking chaos are a common engineering problem [38]. In voltage standards or other applications, both quasiperiodic and chaotic behavior must be avoided; however, surprisingly, the optimum operating region is actually near the onset of chaos. Therefore, further comparative studies of the resonance phenomena in the Frenkel-Kontorova model and other physical systems, particularly experiments, would be very interesting. A comparative study of the chaos in the underdamped FK model and coupled Josephson junction systems is underway and will be published separately.

ACKNOWLEDGMENTS

P.M. and J.T. thank the BLTP, JINR, Dubna, in Russia, for its generous hospitality. This work was supported by the Serbian Ministry of Education and Science under Contracts No. OI-171009 and No. III-45010 and by the Provincial Secretariat for High Education and Scientific Research of Vojvodina (Project No. APV 114-451-2201). The reported study was partially funded by RFBR according to the research projects 15-29-01217.

[1] A. Zettl and G. Grüner, Phys. Rev. B **29**, 755 (1984).
[2] G. Grüner and A. Zettl, Phys. Rep. **119**, 117 (1985).
[3] G. Grüner, Rev. Mod. Phys. **60**, 1129 (1988).
[4] S. Brown and G. Grüner, Sci. Am. **270**, 50 (1994).
[5] R. E. Thorne, J. S. Hubacek, W. G. Lyons, J. W. Lyding, and J. R. Tucker, Phys. Rev. B **37**, 10055 (1988).
[6] R. E. Thorne, W. G. Lyons, J. W. Lyding, J. R. Tucker, and J. Bardeen, Phys. Rev. B **35**, 6348 (1987).
[7] R. E. Thorne, W. G. Lyons, J. W. Lyding, J. R. Tucker, and J. Bardeen, Phys. Rev. B **35**, 6360 (1987).
[8] G. Kriza, G. Quirion, O. Traetteberg, W. Kang, and D. Jerome, Phys. Rev. Lett. **66**, 1922 (1991).
[9] N. Kokubo, R. Besseling, V. M. Vinokur, and P. H. Kes, Phys. Rev. Lett. **88**, 247004 (2002).
[10] C. Reichhardt and C. J. Olson Reichhardt, Phys. Rev. B **92**, 224432 (2015).
[11] A. B. Kolton, D. Domínguez, and N. Grønbech-Jensen, Phys. Rev. Lett. **86**, 4112 (2001).
[12] S. P. Benz, M. S. Rzchowski, M. Tinkham, and C. J. Lobb, Phys. Rev. Lett. **64**, 693 (1990).
[13] H. Sellier, C. Baraduc, F. Lefloch, and R. Calemczuk, Phys. Rev. Lett. **92**, 257005 (2004).
[14] J. U. Free, S. P. Benz, M. S. Rzchowski, M. Tinkham, C. J. Lobb, and M. Octavio, Phys. Rev. B **41**, 7267 (1990).
[15] Yu. M. Shukrinov, S. Yu. Medvedeva, A. E. Botha, M. R. Kolahchi, and A. Irie, Phys. Rev. B **88**, 214515 (2013).
[16] Yu. M. Shukrinov, A. E. Botha, S. Yu. Medvedeva, M. R. Kolahchi, and A. Irie, Chaos **24**, 033115 (2014).
[17] R. C. Dinsmore, III, M.-H. Bae, and A. Bezryadin, Appl. Phys. Lett. **93**, 192505 (2008).
[18] M. H. Bae, R. C. Dinsmore, III, T. Aref, M. Brenner, and A. Bezryadin, Nano Lett. **9**, 1889 (2009).
[19] M. P. N. Juniper, A. V. Straube, R. Besseling, D. G. A. L. Aarts, and R. P. A. Dullens, Nat. Commun. **6**, 7187 (2015).
[20] O. Braun and Yu. S. Kivshar, *The Frenkel-Kontorova Model* (Springer, Berlin, 2003).
[21] J. Tekić and P. Mali, *The ac Driven Frenkel-Kontorova Model* (University of Novi Sad, Novi Sad, 2015).
[22] L. M. Floría and F. Falo, Phys. Rev. Lett. **68**, 2713 (1992).
[23] F. Falo, L. M. Floría, P. J. Martínez, and J. J. Mazo, Phys. Rev. B **48**, 7434 (1993).
[24] L. M. Floría and J. J. Mazo, Adv. Phys. **45**, 505 (1996).
[25] A. Zettl, C. M. Jackson, and G. Grüner, Phys. Rev. B **26**, 5773 (1982).
[26] S. Sridhar, D. Reagor, and G. Grüner, Phys. Rev. Lett. **55**, 1196 (1985).
[27] P. Dubos, H. Courtois, B. Pannetier, F. K. Wilhelm, A. D. Zaikin, and G. Schön, Phys. Rev. B **63**, 064502 (2001).
[28] B. Hu, W.-X. Qin, and Z. Zheng, Physica D **208**, 172 (2005).
[29] J. Tekić and B. Hu, Phys. Rev. E **81**, 036604 (2010).
[30] M. Remoissenet and M. Peyrard, Phys. Rev. B **29**, 3153 (1984).
[31] J. Tekić, P. Mali, Z. Ivić, and M. Pantić, J. Appl. Phys. **114**, 174504 (2013).
[32] R. C. Hilborn, *Chaos and Nonlinear Dynamics* (Oxford University Press, Oxford, 1994).
[33] J. Odavic, P. Mali, and J. Tekić, Phys. Rev. E **91**, 052904 (2015).
[34] P. Bak, Phys. Today **39**(38), 12 (1986).
[35] M. H. Jensen, P. Bak, and T. Bohr, Phys. Rev. Lett. **50**, 1637 (1983).
[36] M. H. Jensen, P. Bak, and T. Bohr, Phys. Rev. A **30**, 1960 (1984).
[37] R. I. Kauz, J. Appl. Phys. **57**, 875 (1985).
[38] R. I. Kauz, Rep. Prog. Phys. **59**, 935 (1996).
[39] W. Press *et al.*, *Numerical Recipes in Fortran 77: The Art of Scientific Computing*, 2nd ed. (Cambridge University Press, Cambridge, 1992).
[40] P. Alstrøm, B. Christiansen, and M. T. Levinsen, Phys. Rev. Lett. **61**, 1679 (1988).
[41] P. Alstrøm, and M. T. Levinsen, Phys. Rev. B **40**, 4609 (1989).
[42] J. Maselko and H. L. Swinney, J. Chem. Phys. **85**, 6430 (1986).
[43] A. Cumming and P. S. Linsay, Phys. Rev. Lett. **59**, 1633 (1987).
[44] S. E. Brown, G. Mozurkewich, and G. Grüner, Phys. Rev. Lett. **52**, 2277 (1984).
[45] A. E. Botha, Yu. M. Shukrinov, and M. R. Kolahchi, Nonlinear Dyn. **84**, 1363 (2016).
[46] J. C. Sprott, *Numerical Calculation of Largest Lyapunov Exponent* (2013), http://sprott.physics.wisc.edu/chaos/lyapexp.htm.

[47] A. Wolf, J. B. Swift, L. Swinney, and J. A. Vastano, Physica D **16**, 285 (1985).
[48] Ch. Skokos, J. Phys. A **34**, 10029 (2001).
[49] P. Benitez, J. C. Losada, R. M. Benito, and F. Borondo, Phys. Rev. E **92**, 042918 (2015).
[50] A. A. Middleton, Phys. Rev. Lett. **68**, 670 (1992).
[51] A. A. Middleton and D. S. Fisher, Phys. Rev. B **47**, 3530 (1993).
[52] A. E. Botha, Yu. M. Shukrinov, S. Yu. Medvedeva, and M. R. Kolahchi, J. Supercond. Nov. Magn. **28**, 349 (2015).